Fermi National Accelerator Laboratory

FERMILAB-Pub-94/001-A
astro-ph/9405036
submitted to *Physical Review D*

MASSIVE TAU NEUTRINO AND SN 1987A

G. Sigl[1,2] and Michael S. Turner[1,2,3]

[1]*Department of Astronomy & Astrophysics*
Enrico Fermi Institute, The University of Chicago, Chicago, IL 60637-1433

[2]*NASA/Fermilab Astrophysics Center*
Fermi National Accelerator Laboratory, Batavia, IL 60510-0500

[3]*Department of Physics, Enrico Fermi Institute*
The University of Chicago, Chicago, IL 60637-1433

ABSTRACT

The emission of MeV-mass tau neutrinos from newly formed neutron stars is considered in a simple, but accurate, model based upon the diffusion approximation. The tau-neutrinosphere temperature is found to increase with mass so that emission of massive tau neutrinos is not suppressed by the Boltzmann factor previously used, $(m_\nu/T_\nu)^{1.5}\exp(-m_\nu/T_\nu)$, where $T_\nu \sim 4\,\mathrm{MeV} - 8\,\mathrm{MeV}$. If the tau neutrino decays to electron neutrinos, then for short lifetimes ($\tau_\nu \lesssim 10^{-3}\,\mathrm{sec}$) the location of both the tau and electron neutrinospheres can be affected, and, for very short lifetimes ($\tau_\nu \lesssim 10^{-6}\,\mathrm{sec}$) its temperature falls below 1 MeV, in conflict with neutrino observations of Supernova 1987A (SN 87A). Using our results, we revise limits to the mass/lifetime of an MeV-mass tau neutrino based upon SN 87A. Our constraints, together with bounds based upon primordial nucleosynthesis and the laboratory mass limit of around 30 MeV, exclude the possibility of a tau neutrino more massive than 0.4 MeV if the dominant decay mode is radiative. Finally, we speculate on the possible role a $15\,\mathrm{MeV} - 25\,\mathrm{MeV}$ tau neutrino might play in the supernova explosion itself.

Operated by Universities Research Association Inc. under contract with the United States Department of Energy

1 Introduction

In most extensions of the standard model neutrinos are massive and unstable. A massive neutrino can decay through standard electroweak interactions into "visible" channels such as $\nu \to \nu'\gamma$ or $\nu \to \nu'\gamma\gamma$, and if it is more massive than about 1 MeV, $\nu \to \nu_e e^+ e^-$ and $\nu \to \nu_e e^+ e^- \gamma$. It can also decay through new interactions into "invisible" channels, e.g., $\nu \to \nu'\phi$ or $\nu \to \nu' + \nu'\bar{\nu}'$, where ϕ is a massless (or very light) boson (e.g., majoron or familon).

Many of the most stringent limits to the radiative decay of a massive neutrino come from the nondetection of a gamma-ray burst coincident with the neutrino burst [1] observed from Supernova 1987A (SN 87A) [2, 3, 4, 5, 6, 7] and from the fact that the energy observed in supernovae in the form of bulk kinetic energy of the expanding envelope and light (about 10^{51} erg in total) are far less than that carried away by a neutrino species (about one third of the the binding energy of a neutron star or 10^{53} erg) [8]. These limits are based on neutrino fluxes calculated within the framework of standard supernova theory where it is assumed that all three standard model neutrino species are massless and stable. The upper limits to the masses of the electron and muon neutrinos, about 7 eV and 250 keV respectively, are much less than the temperature of their neutrinospheres, on the order of 4 MeV and 8 MeV respectively, and so this is certainly a good approximation. The current laboratory limit to the tau-neutrino mass is slightly more than 30 MeV [9] and so such an approximation is not necessarily valid for the tau neutrino. Previously, the mass dependence of the tau-neutrino energy flux has been obtained by simply multiplying the energy flux of a massless neutrino species by a Boltzmann factor, implicitly assuming that the temperature of the tau neutrinosphere does not depend its mass.

Because of the importance of the SN 87A constraints to the tau-neutrino [10], we felt it worth considering more carefully the effect of finite mass and lifetime on the energy fluence of tau neutrinos. To this end, in Sec. 2 we develop a simple model of the transport of MeV-mass tau neutrinos based upon the diffusion approximation. In Sec. 3 we use the tau-neutrino energy fluence calculated in this model to re-derive the constraints that follow from observations of SN 87A.

2 A Simple Model for Tau-neutrino Transport

2.1 Basic considerations

The energy transport within, and the cooling of, a newly born neutron star is predominantly due to neutrinos [11]. Because the neutrino mean free path is very short in a neutron star, it takes neutrinos a few seconds to diffuse from the center of the star to the surface. In considering the transport of tau and mu neutrinos the most important processes are elastic, neutral-current scattering off nucleons, $\nu N \to \nu N$, and pair creation/annihilation processes involving nucleons and $e^\pm$ pairs, $e^\pm \leftrightarrow \nu\bar{\nu}$ and $NN \leftrightarrow NN + \nu\bar{\nu}$. For electron neutrinos charged-current processes involving nucleons and electrons/positrons are also important.

We define the neutrinosphere to be the surface beyond which neutrino number is effectively conserved, i.e., pair creation/annihilation processes have become ineffective and chemical equilibrium ceases to be maintained. Because the elastic-scattering cross section is significantly larger than the corresponding pair creation/annihilation cross sections mu and tau neutrinos continue to scatter off nucleons well beyond the neutrinosphere. However, elastic scatterings conserve neutrino number and approximately conserve neutrino energy, and so they have little effect on the neutrino energy flux. Thus, the flux of mu and tau neutrinos is determined by the conditions at the neutrinosphere.

In passing, we note that the situation for electron neutrinos and antineutrinos is different since they can scatter inelastically through charged-current interactions, e.g., $\nu_e + e^{\pm} \rightarrow \nu_e + e^{\pm}$, $\nu_e + n \rightarrow e^- + p$, or $\bar{\nu}_e + p \rightarrow e^+ + n$. The electron neutrinosphere is very close to the mu/tau neutrinosphere, and in the massless limit the numbers of electron, mu, and tau neutrinos radiated are essentially equal. However, charged-current, inelastic scatterings that take place beyond the neutrinosphere serve to lower the kinetic temperature of electron neutrinos, bringing it closer to the local temperature, ultimately to around 4 MeV. This explains an apparent paradox: namely, how electron neutrinos can be characterized by a temperature that is about a factor of two smaller than mu/tau neutrinos and yet have a fluence that is about the same, rather than a factor of $(T_{\nu_e}/T_{\nu})^3 \sim 1/8$ smaller.

We shall use a simple model based the diffusion approximation to calculate the tau-neutrino energy flux; as mentioned above, diffusion is a very good approximation at the tau neutrinosphere. The location of the tau neutrinosphere involves an interplay between scatterings, pair creation/annihilations, and the local physical conditions (temperature and density). We assume that the underlying physical conditions in the nascent neutron star are the same as those in the standard case (three massless neutrino species). Since, energy transport by tau neutrinos only accounts for about one third of the total energy transport (and doesn't change radically for the masses of interest) this assumption is well motivated. Finally, in actually solving for the flux of tau neutrinos from the neutrinosphere we use a technique akin to the freeze-out approximation used in relic-abundance calculations in the early Universe; by comparison to direct numerical integration of the transport equations we find it to be a very good, time saving approximation.

In the massless limit ($m_{\nu} \ll T_{\nu}$) we find that the temperature of the tau neutrinosphere is 7.5 MeV, in agreement with standard calculations [11]. Further, our results are very insensitive to the input parameters (cross sections, model for physical conditions, and so on), indicating that our various approximations have little effect on the energy flux of tau neutrinos we calculate. Both these facts give us confidence that our model provides reliable results.

2.2 Interactions and physical conditions

In the diffusion approximation the flux of massive tau neutrinos $\phi = -D\nabla n$ where n is the neutrino number density and $D = \lambda v/3$ is the diffusion coefficient, given by the product of the neutrino mean free path λ and velocity v divided by three. Throughout, all energy-

dependent quantities are understood to be averaged over a thermal distribution. Inside the neutrinosphere the temperature is given by the local temperature and outside the neutrinosphere it is taken to be constant and equal to the temperature of the neutrinosphere.

In general, we approximate thermally averaged quantities by a functional form that extrapolates correctly to the ultrarelativistic and nonrelativistic limits; for example,

$$v \approx \left(\frac{3T}{m_\nu + 3T}\right)^{1/2} . \tag{1}$$

Our results are sufficiently robust that the fact that quantities do not have the correct behaviour in the semirelativistic regime is of no consequence.

The diffusion coefficient is given by

$$D(r) = \frac{v}{3 n_{\rm B} \sigma_{\nu {\rm N}}} , \tag{2}$$

where $n_{\rm B}$ is the local baryon number density and $\sigma_{\nu {\rm N}}$ is the cross section for elastic scattering of massive tau neutrinos on nucleons (in a hot, nascent neutron star baryons exist in the form of free nucleons rather than nuclei; see Ref. [11]). We approximate the elastic-scattering cross section by [12]

$$\begin{aligned} v\sigma_{\nu {\rm N}} &\approx \frac{G_{\rm F}^2}{\pi}\left[9T^2 + m_\nu^2\right] \quad \text{Dirac}, \\ v\sigma_{\nu {\rm N}} &\approx \frac{G_{\rm F}^2}{\pi}\left[9T^2 + 5 m_\nu T/2\right] \quad \text{Majorana}, \end{aligned} \tag{3}$$

depending on whether the massive tau neutrino is of the Dirac or of the Majorana type.

We parameterize the physical conditions in the nascent neutron star during its early, very hot phase (first 5 sec − 10 sec) by

$$n_{\rm B}(r) = n_0 \left(\frac{r_0}{r}\right)^k , \quad T(r) = T_0 \left(\frac{n_{\rm B}(r)}{n_0}\right)^{1/3} , \tag{4}$$

where spherical symmetry has been assumed and for the parameters r_0, n_0, T_0 and k we choose

$$r_0 = 30\,{\rm km}, \quad n_0 = 5.97 \times 10^{35}\,{\rm cm}^{-3}, \quad T_0 = 5\,{\rm MeV}, \quad k = 5; \tag{5}$$

see e.g., see Ref. [11]. Our results are insensitive to the precise parameters chosen.

Deep inside a hot neutron star pair creation/annihilation processes involving nucleon neutrino-pair bremsstrahlung dominates those involving $e^\pm$ pairs because of its strong density dependence and the fact that electrons are very degenerate. However, in the important region for our calculation, near the neutrinosphere, the two processes are of comparable importance. We write the total cross section for massive neutrino pair annihilation as their sum,

$$\begin{aligned} \sigma_{\nu\bar\nu} v &\approx \frac{G_{\rm F}^2 a_{NN} n_{\rm B}^2 T^{1/2}/m_N^{5/2}}{9T^2 + 4m_\nu^2/(1 + \pi m_\nu/2T)^{1/2}} + 0.83\frac{G_{\rm F}^2}{\pi}\left[9T^2 + \frac{5}{8}m_\nu^2\right] \quad \text{Dirac}, \\ \sigma_{\nu\bar\nu} v &\approx \frac{G_{\rm F}^2 a_{NN} n_{\rm B}^2 T^{1/2}/m_N^{5/2}}{9T^2 + 4m_\nu^2/(1 + \pi m_\nu/2T)^{1/2}} + 0.83\frac{G_{\rm F}^2}{\pi}\left[9T^2 + \frac{5}{2}m_\nu T\right] \quad \text{Majorana}, \end{aligned} \tag{6}$$

where the numerical constant $a_{NN} \sim 2.93 \times 10^3$. The cross section for the $e^{\pm}$ process is from Ref. [15] and neglects the fact that electrons are mildly degenerate; the cross section for the nucleon bremsstrahlung process is from Refs. [13, 14] and is computed in the dilute-medium approximation which is justified for the highly subnuclear densities around the neutrinosphere.

We also allow for tau-neutrino decays. The rate of neutrino decay and inverse decay is controlled by the neutrino lifetime and energy, with the rate for both processes is reduced by the Lorentz γ factor in the usual way. We take 22.5 MeV to be the typical energy for tau neutrinos and approximate γ by

$$\gamma \approx 1 + \frac{22.5\,\mathrm{MeV}}{m_\nu}. \tag{7}$$

In deriving the transport equation we assume that the daughter products of tau-neutrino decays are in thermal equilibrium so that detailed balance can be used to supply the inverse-decay rate. This assumption is certainly justified if the decay products are ν_e's, ν_μ's, $e^{\pm}$ pairs, or photons and applies to many of the decay processes of interest.

Finally, for the equilibrium number density of a massive tau neutrino we take

$$n_{\mathrm{eq}} \approx \left[\frac{3\zeta(3)}{4\pi^2}T^3(r) + \left(\frac{m_\nu T(r)}{2\pi}\right)^{3/2}\right]\exp\left(-\frac{m_\nu}{T(r)}\right), \tag{8}$$

which extrapolates to the correct form in the ultrarelativistic and nonrelativistic limits.

2.3 Neutrino transport equation

The neutrino transport equation follows from adding pair annihilation/creation and decay/inverse decay to the continuity equation for the neutrino number density

$$\dot{n} + \nabla\phi = -\sigma_{\nu\bar{\nu}} v (n^2 - n_{\mathrm{eq}}^2) - \frac{(n - n_{\mathrm{eq}})}{\gamma\tau_\nu}, \tag{9}$$

where ϕ is the neutrino flux and we have used detailed balance to relate pair creation to pair annihilation and inverse decay to decay.

The use of the diffusion approximation and the assumption of spherical symmetry and stationarity ($\dot{n} = 0$) allows the transport equation to be written as an ordinary second-order, nonlinear differential equation

$$Dn'' + \left(D' + \frac{2}{r}D\right)n' = \sigma_{\nu\bar{\nu}} v (n^2 - n_{\mathrm{eq}}^2) + \frac{(n - n_{\mathrm{eq}})}{\gamma\tau_\nu}, \tag{10}$$

where prime denotes derivative with respect to r.

To solve Eq. (10) two boundary conditions must be specified. To arrive at the first we note that the diffusion approximation breaks down around the surface of last scattering ($r = r_{\mathrm{diff}}$) where neutrinos begin to stream freely out of the star. For $r \gg r_{\mathrm{diff}}$ the flux is therefore

given by $\phi \approx nv/2$ where the factor of two comes from averaging over the angle between the propagation direction and the surface normal. On the other hand, where the diffusion approximation applies ($r \ll r_{\rm diff}$) we have $\phi = -D\nabla n$. Matching these two relations leads to the first boundary condition

$$-D\nabla n\,|_{r_{\rm diff}} = (nv/2)|_{r_{\rm diff}} \ . \tag{11}$$

Now for the second; well inside the neutrinosphere the number density of tau neutrinos is very close to its equilibrium value because annihilation/creation interactions are occurring rapidly. We can therefore linearize Eq. (10) by setting $n = n_{\rm eq}$ in terms that are of zeroth order in the small quantity $(n - n_{\rm eq})$ and solve for n to first order in the deviation from $n_{\rm eq}$. By so doing and solving for $n(r)$ well inside the neutrinosphere we obtain our second boundary condition and Eq. (10) can be integrated outward from this inner boundary. (By varying the position of the inner boundary we have shown that our results do not depend significantly on it, so long as it lies considerably inside the neutrinosphere.)

2.4 The tau neutrinosphere

While we have solved the neutrino transport equation for the flux of massive tau neutrinos by direct numerical integration, we have found that an approximation based upon the "freeze out" of the number of tau neutrinos provides a good approximation that requires far less computational time. In particular, the tau-neutrino energy fluence calculated agrees within about 50%. Given that we are using an approximate model for the nascent neutron star, this accuracy seems adequate.

Recall, at the neutrinosphere the actual neutrino number density begins to differ from its equilibrium value because the mean free path for neutrino pair annihilation/creation becomes too large to maintain equilibrium.[1] To find the neutrinosphere we algebraically solve Eq. (10) for the radius $r_{\rm ns}$ where $n - n_{\rm eq}$ becomes of order unity by setting $n - n_{\rm eq} = n_{\rm eq}$ and $n^2 - n_{\rm eq}^2 = n_{\rm eq}^2$.[2]

$$\left| Dn''_{\rm eq} + \left(D' + \frac{2}{r} D \right) n'_{\rm eq} \right|_{r_{\rm ns}} = \left[v\sigma_{\nu\bar{\nu}} n_{\rm eq}^2 + \frac{n_{\rm eq}}{\gamma\tau} \right]_{r_{\rm ns}} \ . \tag{12}$$

From this, we approximate the power radiated in massive tau-neutrinos,

$$P_\nu(m_\nu \neq 0) \approx [m_\nu + 3T_\nu] 4\pi r_{\rm ns}^2 [Dn'_{\rm eq}]_{r_{\rm ns}} \ , \tag{13}$$

[1] The analogy with the freeze out of a massive particle species in the early Universe is a good one, and the approximate technique we use to solve the transport equation is very similar to the freeze-out approximation used in relic-particle calculations; see Ref. [15].

[2] As it turns out, there is a small mass range where this procedure does not work well because the term on the left-hand side becomes zero. To insure that $r_{\rm ns}$ is a smooth function of m_ν and τ_ν we actually take the maximum of this term and 0.1 times the modulus of an analogous term with a minus sign between the second and the first order derivatives which could otherwise cancel each other.

where $T_\nu \equiv T(r_{\rm ns})$ is the temperature at the tau neutrinosphere. While the power agrees well with the standard results in the massless limit, we shall actually use the ratio of the power for a massive tau neutrino to that of a massless species and the standard results for a massless neutrino species to obtain absolute results for the energy fluence (in any case, the total energy radiated depends upon the cooling time of the hot neutron star). The number fluence of and energy carried by a massless neutrino species (both neutrinos and antineutrinos) are about $1.4 \times 10^{10}\,{\rm cm}^{-2}$ and $10^{53}\,{\rm erg}$ respectively.

Our results for the tau neutrinosphere temperature and tau-neutrino energy fluence are shown in Figs. 1 and 2 as a function of tau neutrino mass and lifetime. In the limit of long lifetime ($t \gtrsim 10^{-2}\,{\rm sec}$) the tau neutrinosphere temperature remains constant at about 7.5 MeV until a mass of about 10 MeV, after which it rises steadily, reaching around 14 MeV for a mass of 100 MeV. The reason for the rise is simple: As the mass increases beyond 10 MeV the tau-neutrino equilibrium abundance at the "massless neutrinosphere" decreases exponentially; pair-annihilation processes vary as the neutrino abundance squared and cannot reduce the neutrino number density to its small equilibrium value for large tau-neutrino masses; thus, the tau neutrinosphere moves inward, to a higher temperature where the abundance is larger. The net result is that the tau-neutrino energy fluence relative to a massless neutrino species decreases far more slowly than it would if one (incorrectly) assumes that the neutrinosphere temperature is independent of neutrino mass; see Fig. 2.

In Figs. 1 and 2 the effect of the tau-neutrino lifetime upon the neutrinosphere is also shown. For lifetimes greater than about $10^{-2}\,{\rm sec}$ there is little effect; as the lifetime is decreased, which corresponds to increasing the rate of decays and inverse decays, the tau-neutrinosphere temperature decreases. The reason is simple: Inverse decays and decays become very effective at maintaining chemical equilibrium, further and further out. In fact, they are so effective that for tau-neutrino lifetimes shorter than about $10^{-3}\,{\rm sec}$ the tau neutrinosphere temperature drops below 7 MeV, and presumably, the electron neutrinosphere temperature is lowered too. For very short lifetimes the effects of decays and inverse decays are so severe that the background model is likely to be affected too, calling into question its validity.

Finally, a brief, but important, comment on the robustness of our results. Consider the tau-neutrinosphere as defined above. Its location depends upon the model of the ambient conditions as well as the rates for elastic scattering and pair-creation/annihilation. Varying the model for the ambient conditions, e.g., k and T_0, affects the tau-neutrinosphere temperature by only a few tenths of an MeV. Likewise, it depends very little upon the overall normalization of the scattering and annihilation rates adopted: In particular, it is the product of the rates that determines T_ν, and changing that product by a factor of ten only changes the tau-neutrinosphere temperature by about 1 MeV and the energy flux by less than a factor of four for long-lived (i.e. $\tau_\nu \gtrsim 0.1\,{\rm sec}$) tau neutrinos. Insensitivity to input parameters is also apparent in the small differences in the results for Dirac and Majorana neutrinos, where the product of the rates differs by a factor $0.1(m_\nu/T_\nu)^2$ for $m_\nu \gtrsim 20\,{\rm MeV}$.

2.5 Wrong-helicity neutrinos

A massive Dirac neutrino has two additional helicity states, ν_R and $\bar{\nu}_L$, which in the absence of new interactions only interact by virtue of the mismatch between chirality and helicity. For every ordinary process, e.g., $\nu_L + N \to \nu_L + N$, there is a spin-flip analog, here, $\nu_L + N \to \nu_R + N$, which is suppressed by a factor of $(m_\nu/2E_\nu)^2$.

For masses much less than 1 MeV the suppression factor is very large and the mean-free path of a wrong-helicity neutrino is much larger than the radius of a neutron star. Wrong-helicity neutrinos that are produced simply stream out, tending to accelerate the cooling of a hot neutron star, e.g., the one associated with SN 87A, and thereby shortening the duration of the predicted neutrino signal. The duration of the neutrino burst observed by KII and IMB has been used to exclude a Dirac neutrino of mass between about 10 keV and 1 MeV [16].

For masses much greater than 1 MeV the suppression factor is not significant, and wrong-helicity neutrinos become trapped and are radiated from a "wrong-helicity" neutrinosphere. Using our diffusion model we have estimated the location of the wrong-helicity neutrinosphere. (The dominant interactions for both scattering and creation/destruction are spin-flip neutrino-nucleon scatterings; see Ref. [13].) For a mass of 1 MeV the wrong-helicity neutrinosphere temperature is about 40 MeV, and wrong-helicity neutrinos will quickly rob the core of the hot neutron star of most of its thermal reserves. As before, this is excluded by the KII and IMB data. As the mass increases the temperature of the wrong-helicity neutrinosphere decreases, reaching a temperature comparable to that of the proper-helicity neutrinosphere for $m_\nu = 5\,\mathrm{MeV}$. For $m_\nu \gg 5\,\mathrm{MeV}$ both neutrinospheres coincide, thereby roughly doubling the energy flux (compared to a Majorana neutrino).

The two neutrinospheres are coupled (through spin-flip interactions); to properly take account of both helicity states of an MeV Dirac neutrino is beyond the scope of this study. Since we are only interested in neutrino masses greater than a few MeV, where wrong-helicity neutrinos carry off only about as much energy as proper-helicity neutrinos, to be conservative we simply ignore the energy carried off by wrong-helicity neutrinos. (Doubling our energy fluxes would change our results very little.)

3 Constraints Based Upon SN 87A

In this Section we re-examine the important mass-lifetime limits to an MeV-mass tau neutrino based on SN 87A using the more accurate tau-neutrino fluence computed here. In general, our limits are significantly more stringent as the tau-neutrino energy fluence is larger than had previously been assumed. The limits we discuss are based upon three observations: (i) the total "visible" energy, the kinetic energy of the expanding shell of matter (about 10^{51} erg) and the optical light output (about 10^{49} erg), was less than 10^{51} erg [17]; (ii) the gamma-ray fluence around the time when the neutrinos were detected was very small compared to the enormous neutrino fluence, $F_\nu \sim 10^{10}\,\mathrm{cm}^{-2}$ [3]; and (iii) 19 neutrino events were detected by the KII and IMB detectors [1], consistent with antielectron neutrinos emit-

ted with a kinetic temperature of about 4 MeV [11]. In deriving our mass-lifetime limits for a tau neutrino of mass greater than a few MeV, we follow closely the treatments in Refs. [7, 18] and also assume that the decay rate is dominated by visible channels (i.e., daughter products include photons or $e^{\pm}$ pairs).

3.1 Decays inside the progenitor

The progenitor of SN 87A had a size of about 3×10^{12} cm [17]. For tau-neutrino lifetimes of the order 100 sec or smaller an appreciable fraction of the tau neutrinos emitted decay inside the progenitor and deposit energy. Since both $e^{\pm}$ pairs and photons have small mean free paths inside the progenitor and thus should deposit all their energy within the envelope of the progenitor, our arguments do not depend whether the daughter products are $e^{\pm}$ pairs or photons. The fraction of tau neutrinos that decay inside the progenitor

$$f_{\rm inside} = 1 - \exp(-t_{\rm inside}/\tau_L), \tag{14}$$

where $t_{\rm inside} \approx 100\,{\rm sec}/v$ is the time it takes a tau neutrino to escape the progenitor and $\tau_L = \gamma\tau_\nu$ is the lifetime in the progenitor rest frame.

We demand that the energy deposited inside the progenitor $E_{\rm inside}$ be less than about 10^{51} erg to be consistent with the observations of SN 87A (and other type II supernovae):

$$E_{\rm inside} \approx f_{\rm inside} 10^{53}\,{\rm erg} \left(\frac{P_\nu(m_\nu \neq 0)}{P_\nu(m_\nu = 0)}\right) \lesssim 10^{51}\,{\rm erg}. \tag{15}$$

The region of the mass-lifetime plane excluded by this consideration is shown in Fig. 3 (labeled SNL).

3.2 Decays outside the progenitor

The differential gamma-ray fluence at Earth due to tau-neutrino decays via the channel $\nu_\tau \to \nu_e\gamma$ was calculated in Ref. [7]. As modified to our approximations it is

$$\frac{dF_\gamma}{dE_\gamma} = \frac{B_\gamma F_\nu E_\gamma}{T_\nu m_\nu \tau_\nu} \left(\frac{r_{\rm ns}}{r_{\rm rel}}\right)^2 \int_0^{t_{\rm max}} dt \exp(-2E_\gamma t/m_\nu\tau_\nu) \left(1 + \frac{E_{\rm min}}{T_\nu}\right) \exp(-E_{\rm min}/T_\nu)\,, \tag{16}$$

where $r_{\rm ns}$ and T_ν are the radius and temperature of the tau neutrinosphere respectively, $r_{\rm rel}$ is the radius of the light neutrinosphere, $E_{\rm min}$ is the maximum of E_γ and

$$m_\nu \left[1 + (100\,{\rm sec} \cdot m_\nu/2E_\gamma t)^{1/2}\right],$$

and $t_{\rm max} = 223.2\,{\rm sec}$ is the time interval over which the authors of Ref. [7] analysed the data recorded by the Gamma-Ray Spectrometer on board the Solar Maximum Mission satellite. Eq. (16) differs from the original expression in Ref. [7] in two respects: First, the neutrinosphere temperature T_ν depends upon tau-neutrino mass; and second, the tau-neutrino

fluence is must be modified by the geometrical factor $(r_{\rm ns}/r_{\rm rel})^2$ relative to the light neutrino fluence $F_\nu = 1.4 \times 10^{10}\,{\rm cm}^{-2}$.

In this case we are only interested in decays that produce a gamma ray. However, for MeV-mass tau neutrinos the mode $\nu_\tau \to \nu + e^\pm$ is kinematically allowed and likely dominates the photonic mode. Assuming it proceeds via standard electroweak interactions,

$$\tau_\nu = \frac{192\pi^3}{G_F^2 m_\nu^5 \sin^2\theta\cos^2\theta} \simeq \frac{1\,{\rm sec}}{\sin^2 2\theta (m_\nu/10\,{\rm MeV})^5}\,, \tag{17}$$

where θ is the $\nu_\tau - \nu_e$ mixing angle. To wit, we have taken the factor $B_\gamma \sim 10^{-3}$, corresponding to the fraction of decays expected to have a bremsstrahlung photon (also see Ref. [21]). Integrating Eq. (16) over the suitable energy bands and comparing with the corresponding 3σ fluence limits reported in Ref. [7] leads to the excluded region denoted SMM in Fig. 3 [20].

3.3 SN 87A neutrinos

The nineteen neutrino events recorded by the KII and IMB detectors confirmed the standard model of the cooling of a nascent neutron star and had an energy distribution consistent with a temperature of about 4 MeV [11]. As noted earlier and illustrated in Figs. 2b and 2c, for very short lifetimes ($\tau_\nu \lesssim 10^{-6}\,{\rm sec}$), decays and inverse decays become so potent that they move the tau and electron neutrinospheres outward to a region where the temperature is around 1 MeV or less. Clearly this is inconsistent with the KII and IMB data. However, we hasten to add that our model for the neutrinosphere is not self consistent under such extreme conditions. More importantly, lifetimes for the modes $\nu_\tau \to \nu_e + e^\pm$ or $\nu_\tau \to \nu + \gamma$ shorter than about 1 sec are excluded by data from the Big European Bubble Chamber (BEBC) experiment [19] (shown in Fig. 3). Unless new interactions beyond the standard model can give rise to a very short lifetime for a nonelectromagnetic mode where all the daughter products would be in thermal equilibrium in a hot neutron star, it would seem that our results for very short lifetimes are without application.

In passing we mention that if tau neutrinos decay beyond the electron neutrinosphere, corresponding to $\tau_\nu \gtrsim 10^{-3}\,{\rm sec}$, there is an additional population of antielectron neutrinos, which for $m_\nu \lesssim 10\,{\rm MeV}$ is of comparable importance. It appears unlikely that our understanding of SN 87A and the KII/IMB data are good enough to exclude this possibility. However, because MeV-mass neutrinos are only semi-relativistic, these additional events would be characterized by a time delay/spread on the order of the tau-neutrino lifetime itself and thus could perhaps be excluded (or confirmed) on that basis. (In fact, it could be wildly speculated that a tau neutrino with a lifetime of seconds and a mass of 1 MeV – 10 MeV could be responsible for the second cluster of KII events.)

3.4 Residual annihilations

Finally, we would like to draw attention to an interesting aspect of the behaviour of the numerical solutions of Eq. (10) in the long-lifetime limit. In Figs. 4 we show the solution and

the equilibrium distribution for the massless case and for $m_\nu = 30\,\mathrm{MeV}$. The departure from equilibrium near the neutrinosphere radius is clearly visible. The kinks mark the surface of last scattering ($r = r_{\mathrm{diff}}$) where the boundary condition Eq. (11) applies. In the massless case the actual tau-neutrino number density "undershoots" the equilibrium density in the diffusion region, whereas in the massive case it "overshoots." The "overshoot effect" suggests that a massive neutrino could be effective in depositing energy into the outer core region by residual annihilations and thus could help power the supernova explosion itself. (At present, it is not understood precisely how the explosion is powered [11, 17]).

To study this further we calculated the energy deposited in the region between the light neutrinosphere and the outer boundary of the diffusion region. (Inside the light neutrinosphere any energy deposited will be radiated in electron/muon neutrinos, and beyond the diffusion region annihilations are totally ineffective because of the free streaming of neutrinos). We approximate this energy by

$$E_{\nu\bar{\nu}} \sim (m_\nu + 3T_\nu) \int_{r_{\mathrm{rel}}}^{r_{\mathrm{diff}}} 4\pi r^2 dr \sigma_{\nu\bar{\nu}} v \left(n^2 - n_{\mathrm{eq}}^2\right) , \tag{18}$$

where $\sigma_{\nu\bar{\nu}} v$ is evaluated at the tau neutrinosphere and $n(r)$ is the analytical solution of Eq. (10) between r_{ns} and r_{diff} for vanishing right-hand side and $D(r) = D(r_{\mathrm{ns}})(r/r_{\mathrm{ns}})^k$. In Fig. 5 we show the ratio of the energy deposited to the energy carried off by a massless neutrino species (about $10^{53}\,\mathrm{erg}$). For tau-neutrino masses between about 15 MeV and 25 MeV the energy deposited is about $10^{51}\,\mathrm{erg}$, which is comparable to the energy seen in the kinetic motion of the explosion and thus could have an important effect on the supernova explosion—perhaps solving the riddle of the explosion itself.

4 Concluding Remarks

We have studied the transport of energy by MeV-mass tau neutrinos during the early cooling phase of a hot neutron star. By means of a simple, but accurate, diffusion model we have computed the energy fluence and neutrinosphere temperature. Because the neutrinosphere temperature increases with tau-neutrino mass the energy carried off by massive tau neutrinos does not decrease nearly as rapidly as it would if the tau-neutrinosphere temperature were independent of mass, as previously assumed. (We mention that our method could easily be generalized to calculate the flux of hypothetical, massive particles with interactions whose strength is roughly weak—e.g., new particles predicted in supersymmetric models—if the motivation should arise.)

Using these new results we have re-derived the mass-lifetime bounds that follow from SN 87A. Based upon SMM gamma-ray data we exclude a massive tau neutrino of lifetime shorter than about $10^8\,\mathrm{sec}$ whose decays are radiative. This, taken with the recent bounds based upon primordial nucleosynthesis [18, 22], excludes a tau neutrino more massive than about 0.4 MeV regardless of its lifetime, provided only that its decays are radiative. In addition, a Dirac tau neutrino of mass from about 10 keV to 1 MeV is excluded on the basis of the fact that wrong-helicity tau-neutrinos produced deep in the core would have carried off too

much energy, leading to an unacceptably short burst of antielectron neutrinos [16]. Finally, we speculate that a tau neutrino of mass 15 MeV – 25 MeV could play an important role in the supernova explosion process itself by virtue of the energy its annihilations deposit just outside the tau neutrinosphere.

Acknowledgments

We thank Adam Burrows, Scott Dodelson and David Seckel for helpful comments. This work was supported in part by the Department of Energy (at Chicago and at Fermilab), by the NASA through grant NAGW-2381 (at Fermilab) and by the Alexander-von-Humboldt Foundation.

References

[1] K. Hirata et al., *Phys. Rev. Lett.* **58**, 1490 (1987); R.M. Bionta et al., *ibid*, 1494.

[2] F. Von Feilitzsch and L. Oberauer, *Phys. Lett.* **B200**, 580 (1988).

[3] E. L. Chupp, W. F. Vestrand and C. Repping, *Phys. Rev. Lett.* **62**, 505 (1989).

[4] E.W. Kolb and M.S. Turner, *Phys. Rev. Lett.* **62**, 509 (1989).

[5] S. A. Bludman, *Phys. Rev.* **D45**, 4720 (1992).

[6] J.M. Soares and L.M. Wolfenstein, *Phys. Rev. D* **40**, 3666 (1989); *Phys. Rev. Lett.* **64**, 1310 (1990).

[7] L. Oberauer, C. Hagner, G. Raffelt and E. Rieger, *Astropart. Phys.* **1**, 377 (1993).

[8] S.W. Falk and D.N. Schramm, *Phys. Lett. B* **79**, 511 (1978); R. Cowsik, D.N. Schramm, and P. Hoflich, *Phys. Lett. B* **218**, 91 (1989).

[9] D. Cinabro et al. (CLEO Collaboration), *Phys. Rev. Lett.* **70**, 3700 (1993); H. Albrecht et al. (ARGUS Collaboration), *Phys. Lett. B* **292**, 221 (1992).

[10] See e.g., A. Dar and S. Dado, *Phys. Rev. Lett.* **59**, 2368 (1987); L. Oberauer, C. Hagner, G. Raffelt and E. Rieger, *Astropart. Phys.* **1**, 377 (1993); K.S. Babu, T.M. Gould, and I.Z. Rothstein, *Phys. Lett. B* **321**, 140 (1994); R.N. Mohapatra, S. Nussinov, and X. Zhang, *Phys. Rev. D* **49**, 3434 (1994); S. Dodelson, G. Gyuk, and M.S. Turner, *ibid*, in press (1994).

[11] A. Burrows, *Ann. Rev. Nucl. Part. Sci.* **40**, 181 (1990) and references therein.

[12] D.L. Tubbs and D.N. Schramm, *Astrophys. J.* **201**, 467 (1975); S. W. Bruenn and W. C. Haxton, *ibid* **376**, 678 (1991).

[13] M.S. Turner, *Phys. Rev. D* **45**, 1066 (1992).

[14] G. G. Raffelt and D. Seckel, Report MPI-Ph/93-90 BA-93-43.

[15] E.W. Kolb and M.S. Turner, *The Early Universe* (Addison-Wesley, Redwood City, CA, 1990), Ch. 5.

[16] A. Burrows, R. Gandhi, and M.S. Turner, *Phys. Rev. Lett.* **68**, 3834 (1992); R. Mayle, D.N. Schramm, M.S. Turner, and J. Wilson, *Phys. Lett. B* **317**, 119 (1993); S. Dodelson, J.A. Frieman, and M.S. Turner, *Phys. Rev. Lett.* **68**, 2572 (1992); and references therein.

[17] W.D. Arnett et al., *Ann. Rev. Astron. Astrophys.* **27**, 629 (1989).

[18] S. Dodelson, G. Gyuk, and M.S. Turner, *Phys. Rev. D*, in press (1994).

[19] A.M. Cooper-Sarkar et al., *Phys. Lett. B* **160**, 207 (1985); K.S. Babu, T.M. Gould, and I.Z. Rothstein, *Phys. Lett. B* **321**, 140 (1994).

[20] Another, possibly more stringent, limit based upon SN 87A follows the analysis of data from a gamma-ray detector on the late Pioneer Venus Orbiter (PVO); A. Jaffe and M.S. Turner, work in preparation (1993).

[21] R.N. Mohapatra, S. Nussinov, and X. Zhang, *Phys. Rev. D* **49**, 3434 (1994). These authors also suggest other ways, besides the expected branching ratio of 10^{-3} due to radiative corrections, in which decay-produced $e^{\pm}$ might produce photons.

[22] M. Kawasaki et al., *Nucl. Phys. B* **419**, in press (1994).

Figure Captions

Figure 1: Tau-neutrinosphere temperature as a function of tau-neutrino mass: (a) Long-lifetime limit (upper curves) and $\tau_\nu = 10^{-5}$ sec (lower curves) for Dirac (solid) and Majorana (broken) mass; (b) Contours in the mass-lifetime plane for Dirac mass; and (c) Contours in the mass-lifetime plan for Majorana mass. Contours are in steps of 0.5 MeV beginning with 7.5 MeV in the upper left corner. The temperature increases to the right and decreases to the bottom.

Figure 2: Massive tau-neutrino energy flux relative to a massless tau neutrino: (a) Long-lifetime limit (upper curves) and $\tau_\nu = 10^{-5}$ sec (lower curves) for Dirac (solid) and Majorana (broken) mass compared to the naive Boltzmann suppression factor for mass-independent neutrinosphere temperature $T_\nu = 7.5$ MeV (dotted); (b) Contours in the mass-lifetime plane for Dirac mass; and (c) Contours in the mass-lifetime plane for Majorana mass. Flux contours decrease by a factor of 10 (per contour) from top left to the lower right.

Figure 3: Excluded regions of the tau-neutrino mass-lifetime plane: (a) Dirac mass; and (b) Majorana mass. Forbidden regions are on the same side as the label; SNL is the limit based upon decays inside the progenitor; SMM is the limit based upon decays outside the progenitor and the excluded region is between the curve just above SMM and the unmarked lower curve; CLEO/ARGUS refers to the laboratory mass limit; and BEBC refers to the laboratory lifetime limit discussed in Sec. 3.3.

Figure 4: Numerical solution for tau-neutrino number density (solid curve) and equilibrium number density (broken curve), both relative to the neutrino number density at the inner boundary (see Sec. 2.3): (a) massless tau neutrino; and (b) 30 MeV Dirac tau neutrino.

Figure 5: Energy deposited by residual annihilations of a tau neutrino as a function of tau-neutrino mass in units of 10^{53} erg; solid curve is for Dirac and broken curve is for Majorana.

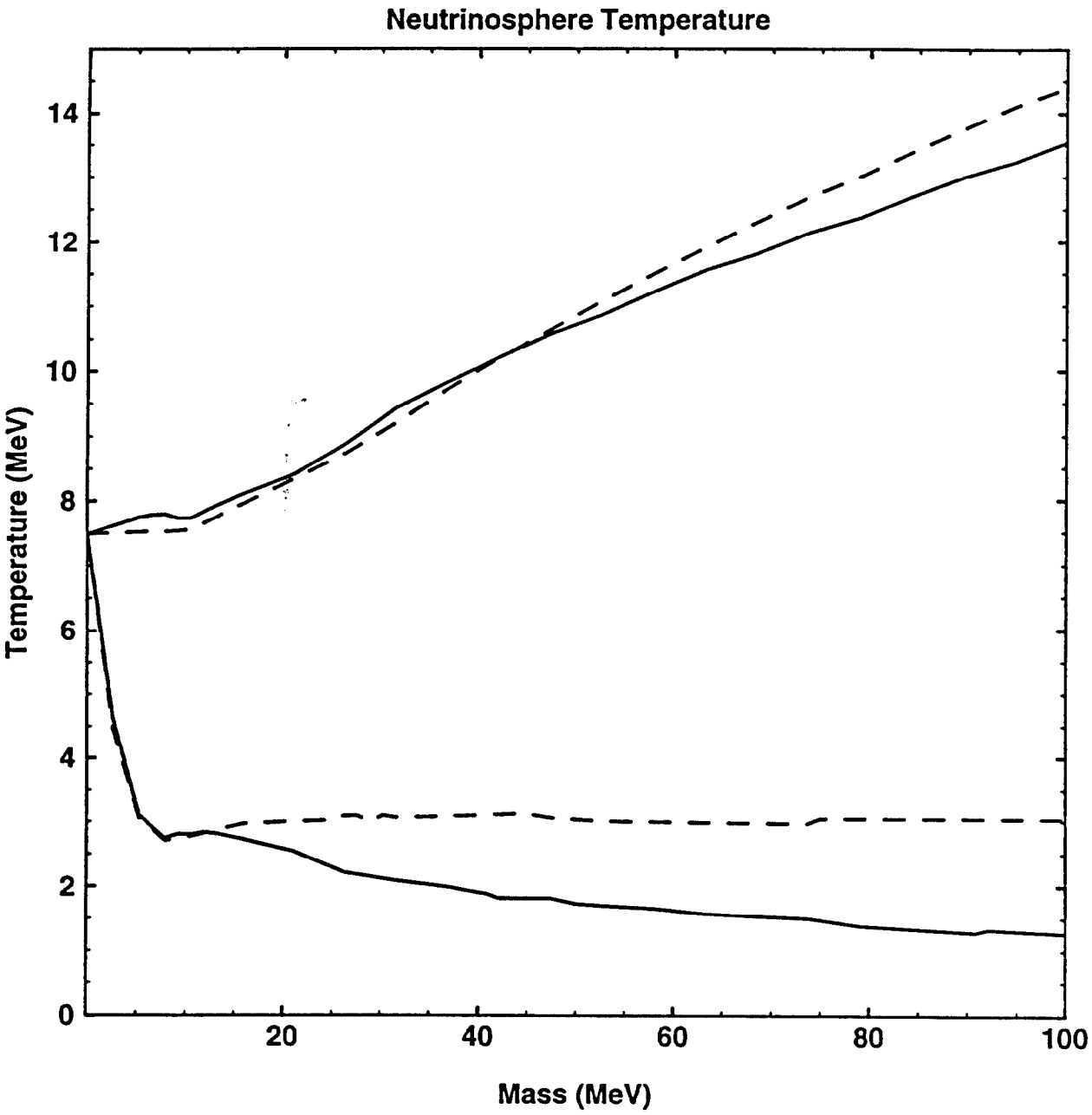
Neutrinosphere Temperature
Temperature (MeV)
0
2
4
6
8
10
12
14
20
40
60
80
100
Mass (MeV)

FIG 1A

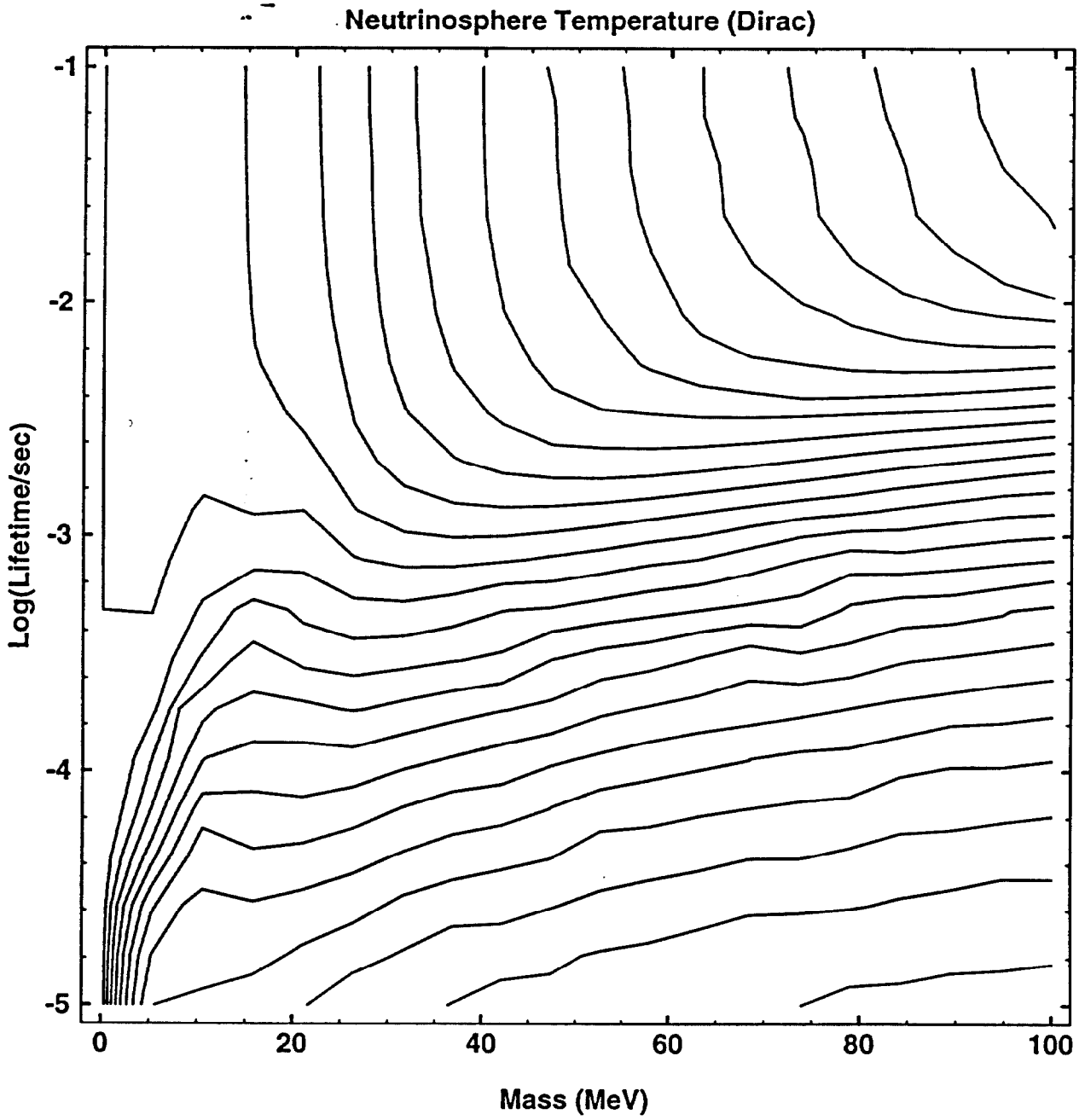
Neutrinosphere Temperature (Dirac)
Log(Lifetime/sec)
-1
-2
-3
-4
-5
0
20
40
60
80
100
Mass (MeV)

FIG 1B

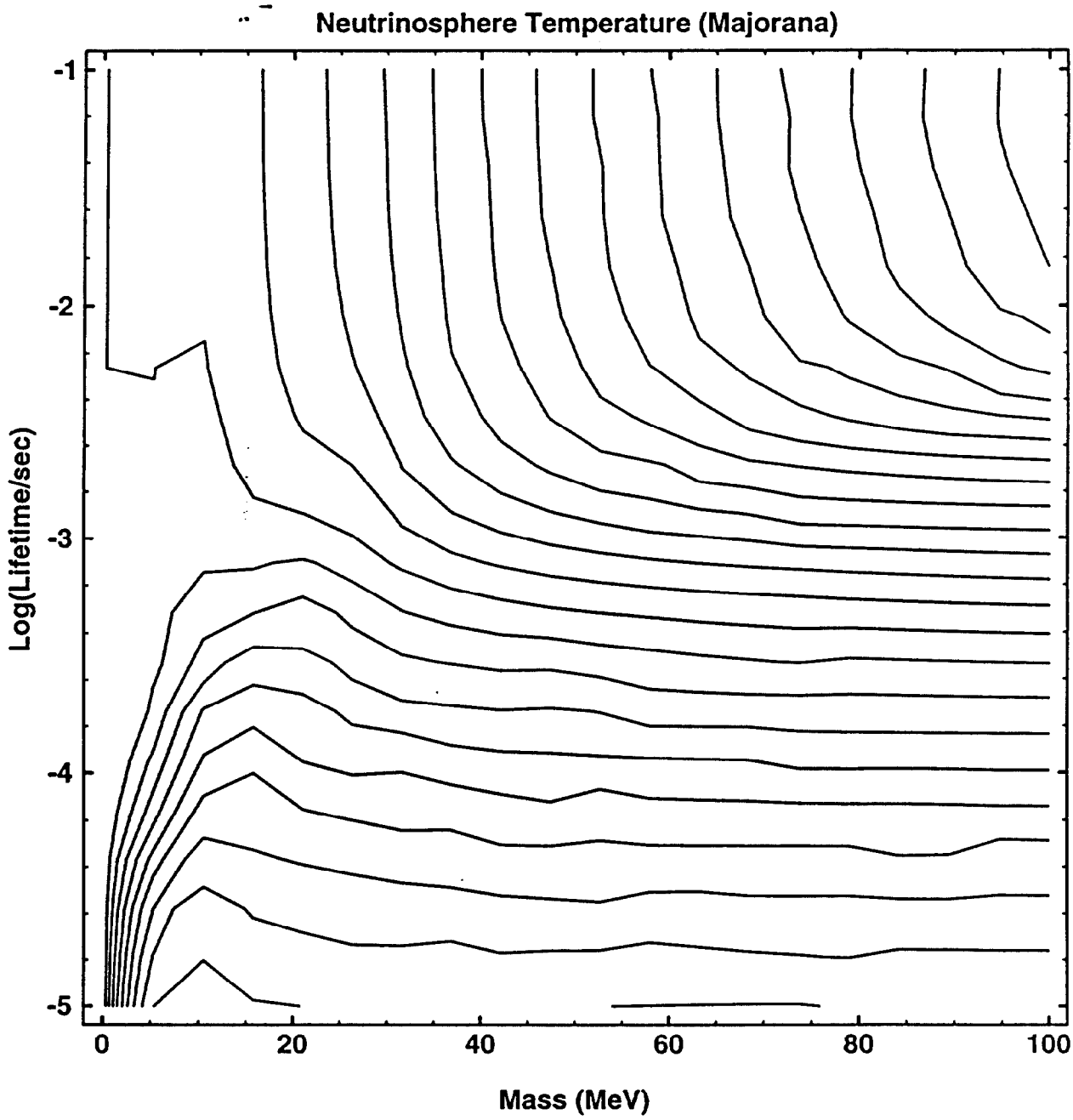
Neutrinosphere Temperature (Majorana)
Log(Lifetime/sec)
-1
-2
-3
-4
-5
0
20
40
60
80
100
Mass (MeV)

FIG 1C

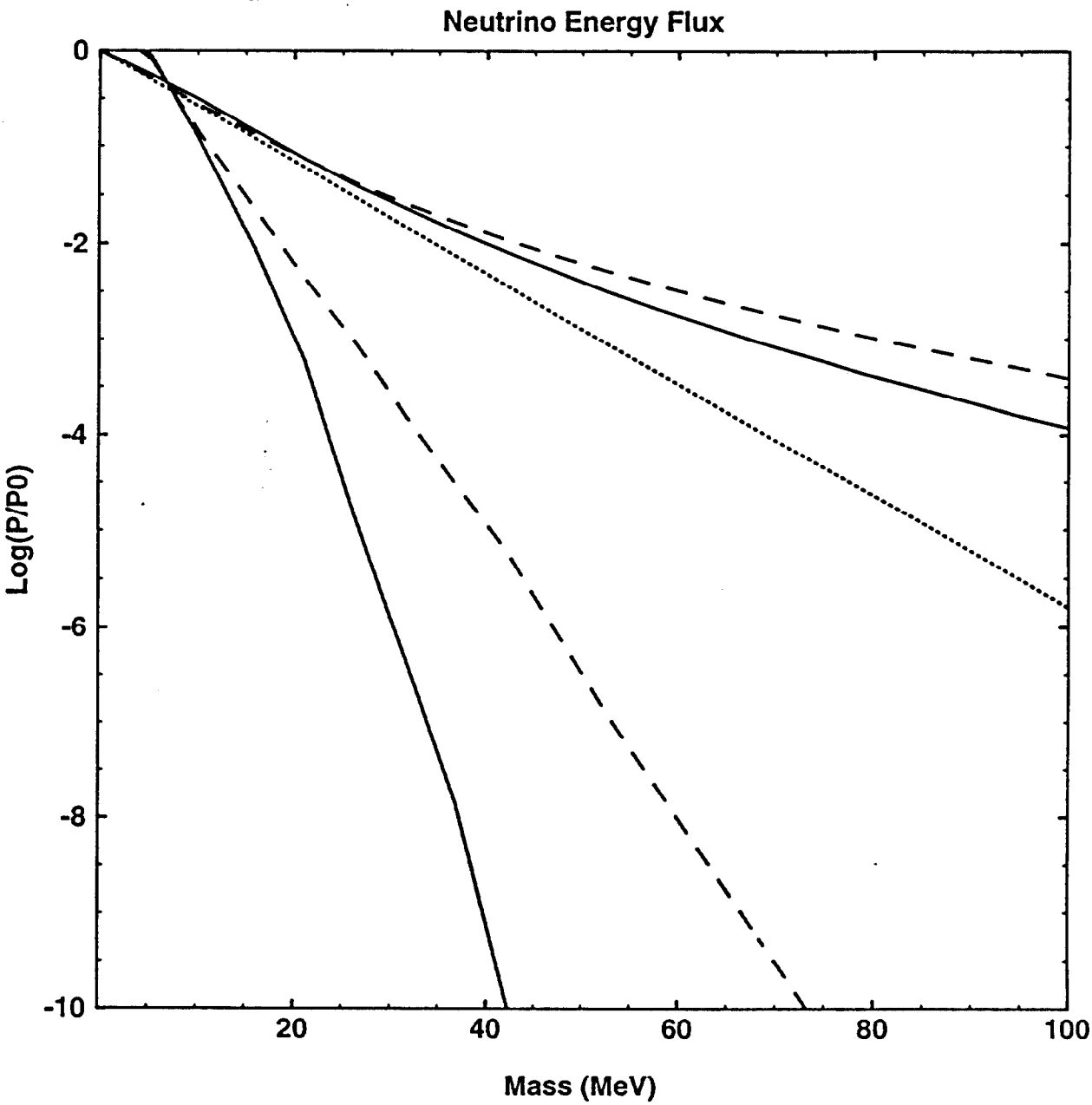

FIG 2A

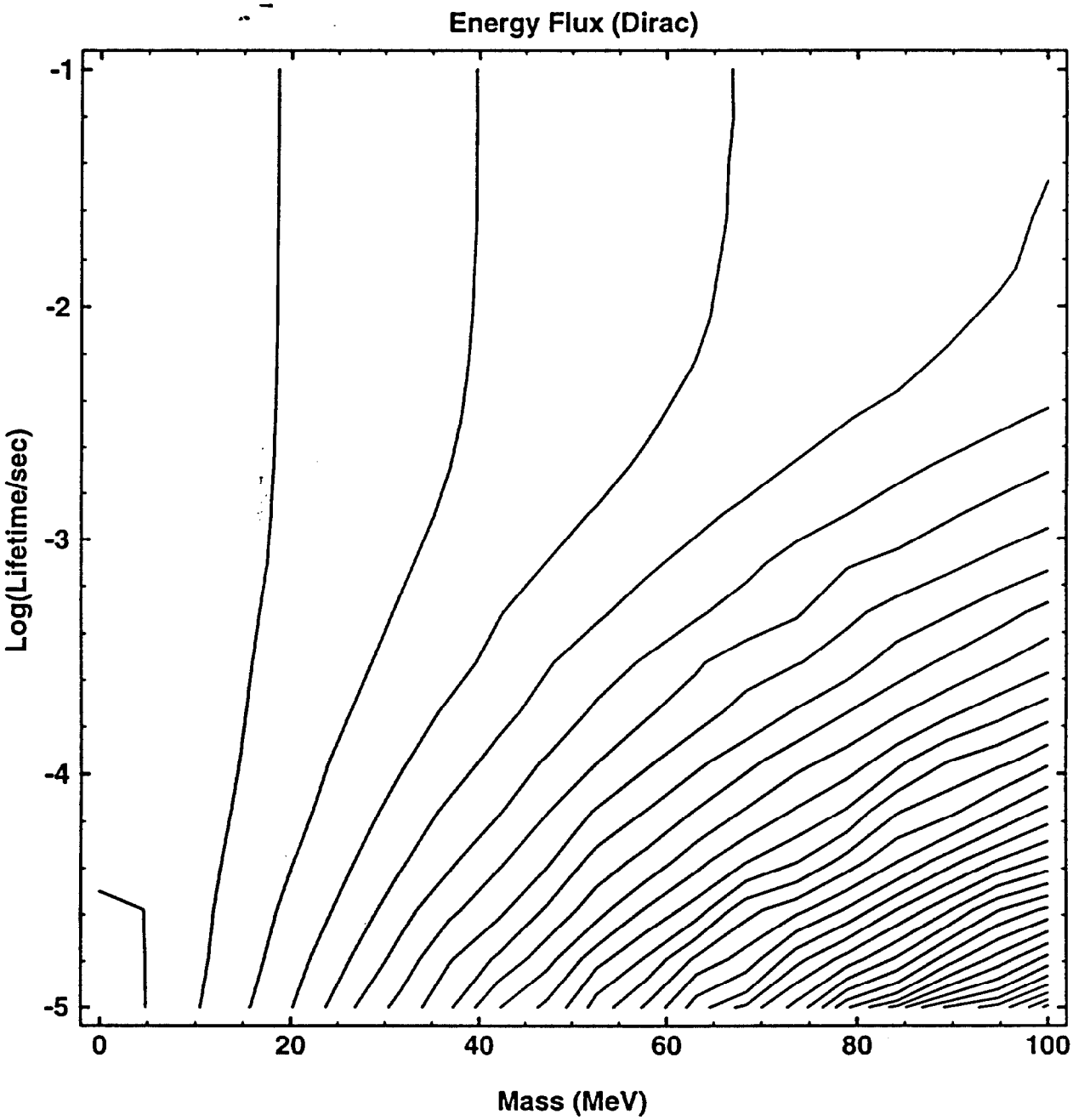
Energy Flux (Dirac)
Log(Lifetime/sec)
-1
-2
-3
-4
-5
0
20
40
60
80
100
Mass (MeV)

FIG-2B

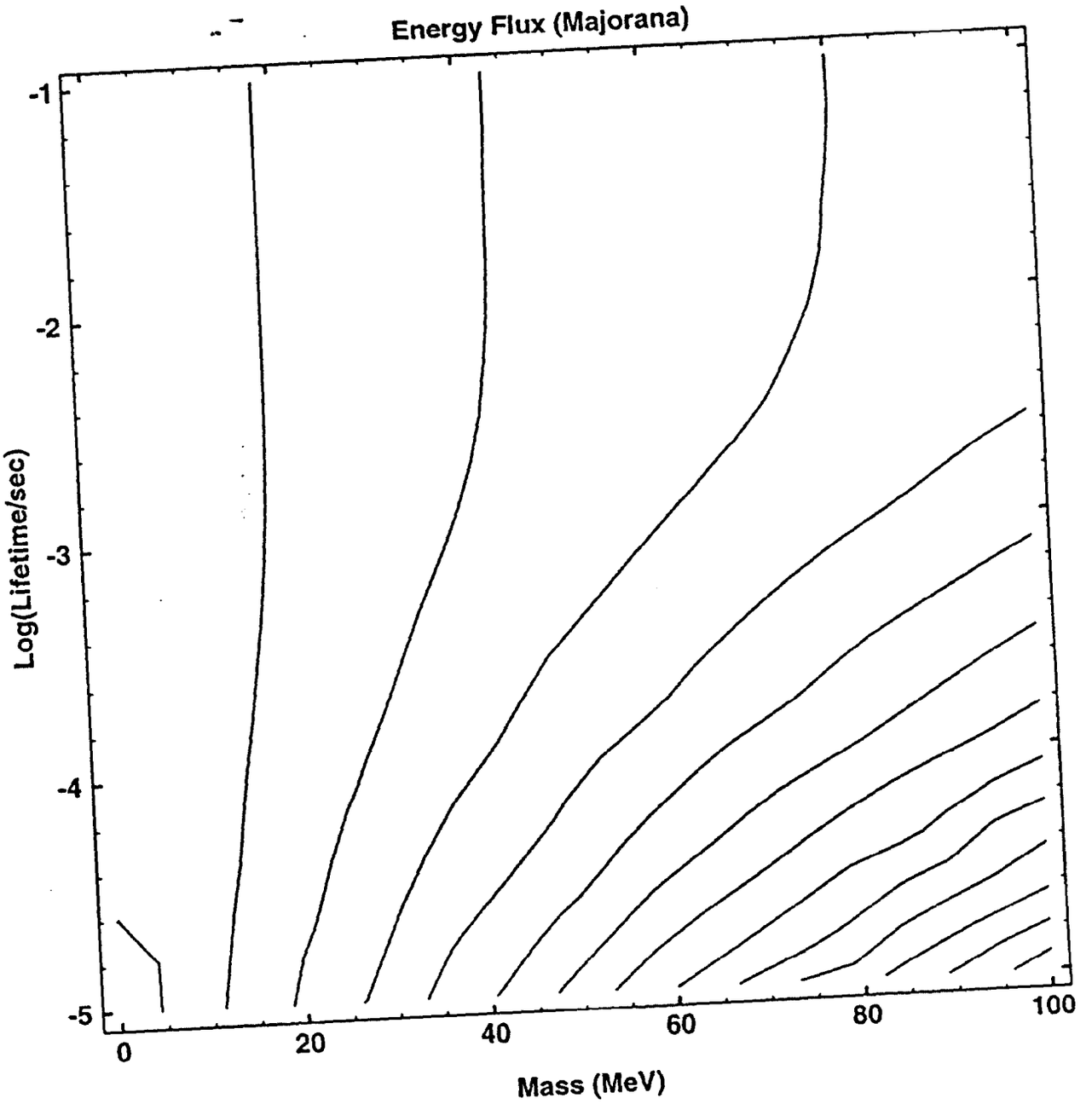
Energy Flux (Majorana)
Log(Lifetime/sec)
-1
-2
-3
-4
-5
0
20
40
60
80
100
Mass (MeV)

FIG 2C.

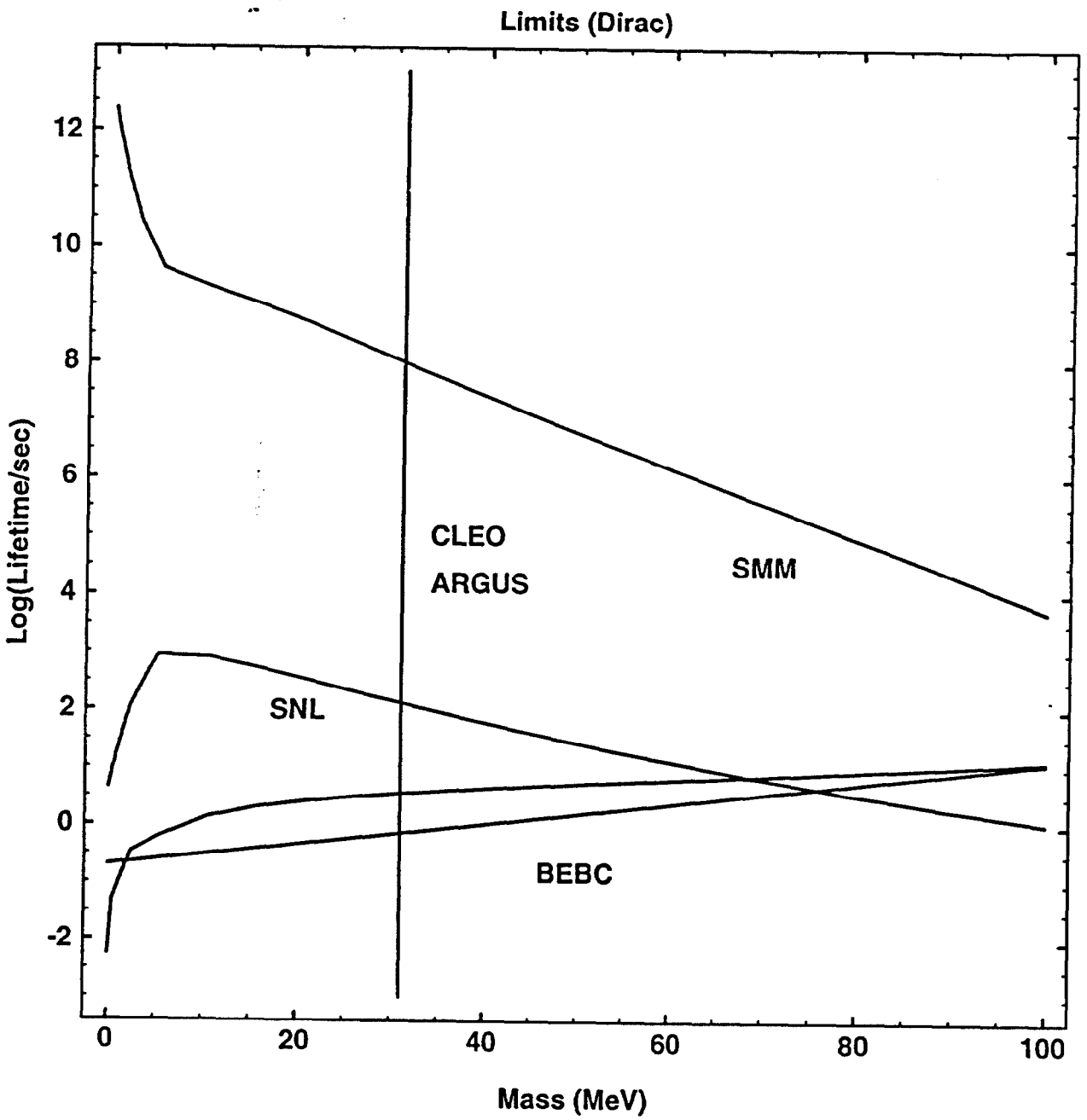
Limits (Dirac)
Log(Lifetime/sec)
12
10
8
6
4
2
0
-2
0
20
40
60
80
100
Mass (MeV)
CLEO
ARGUS
SMM
SNL
BEBC

FIG-3A

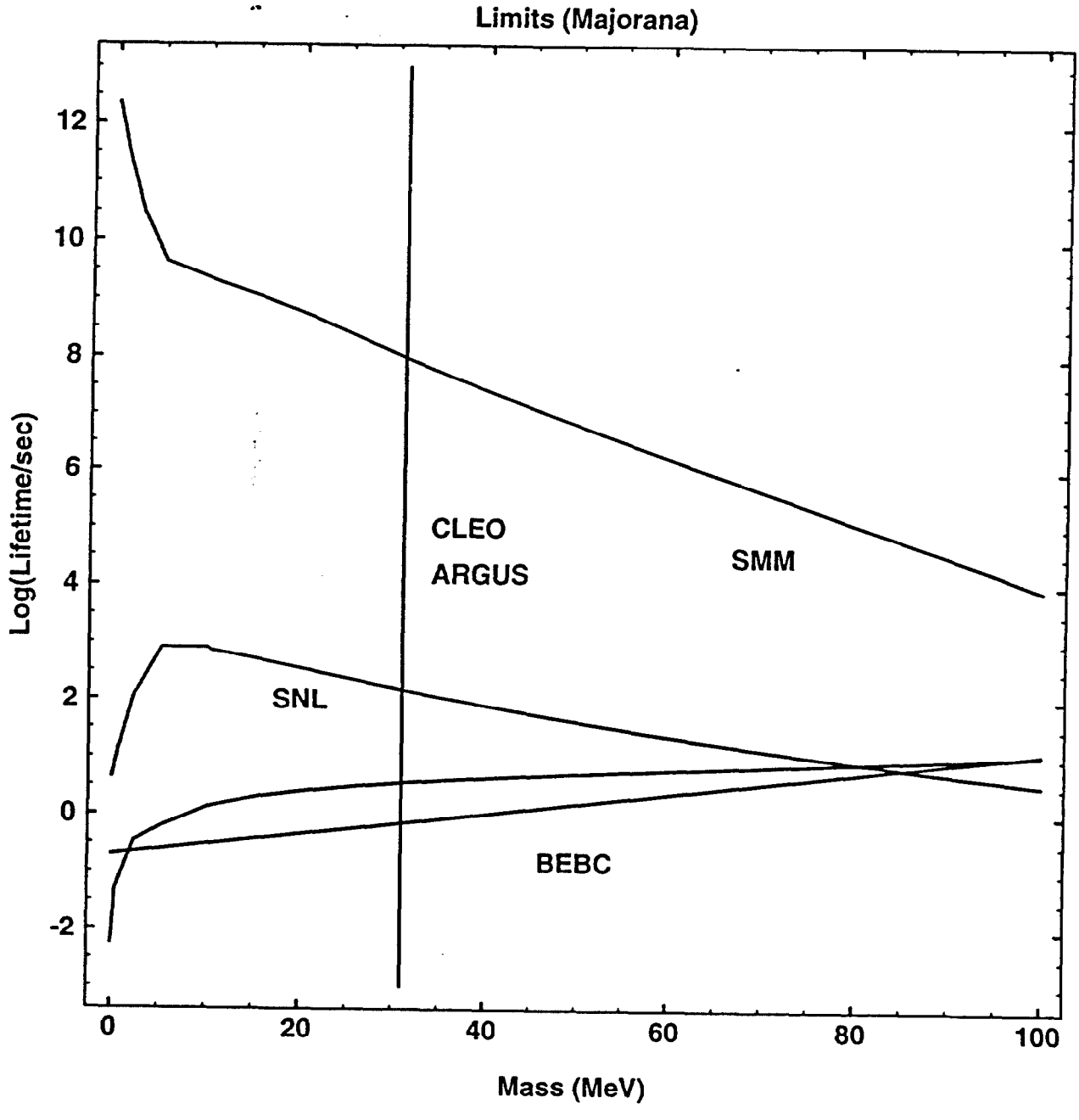
Limits (Majorana)
Log(Lifetime/sec)
12
10
8
6
4
2
0
-2
0
20
40
60
80
100
Mass (MeV)
CLEO
ARGUS
SMM
SNL
BEBC

FIG-3B

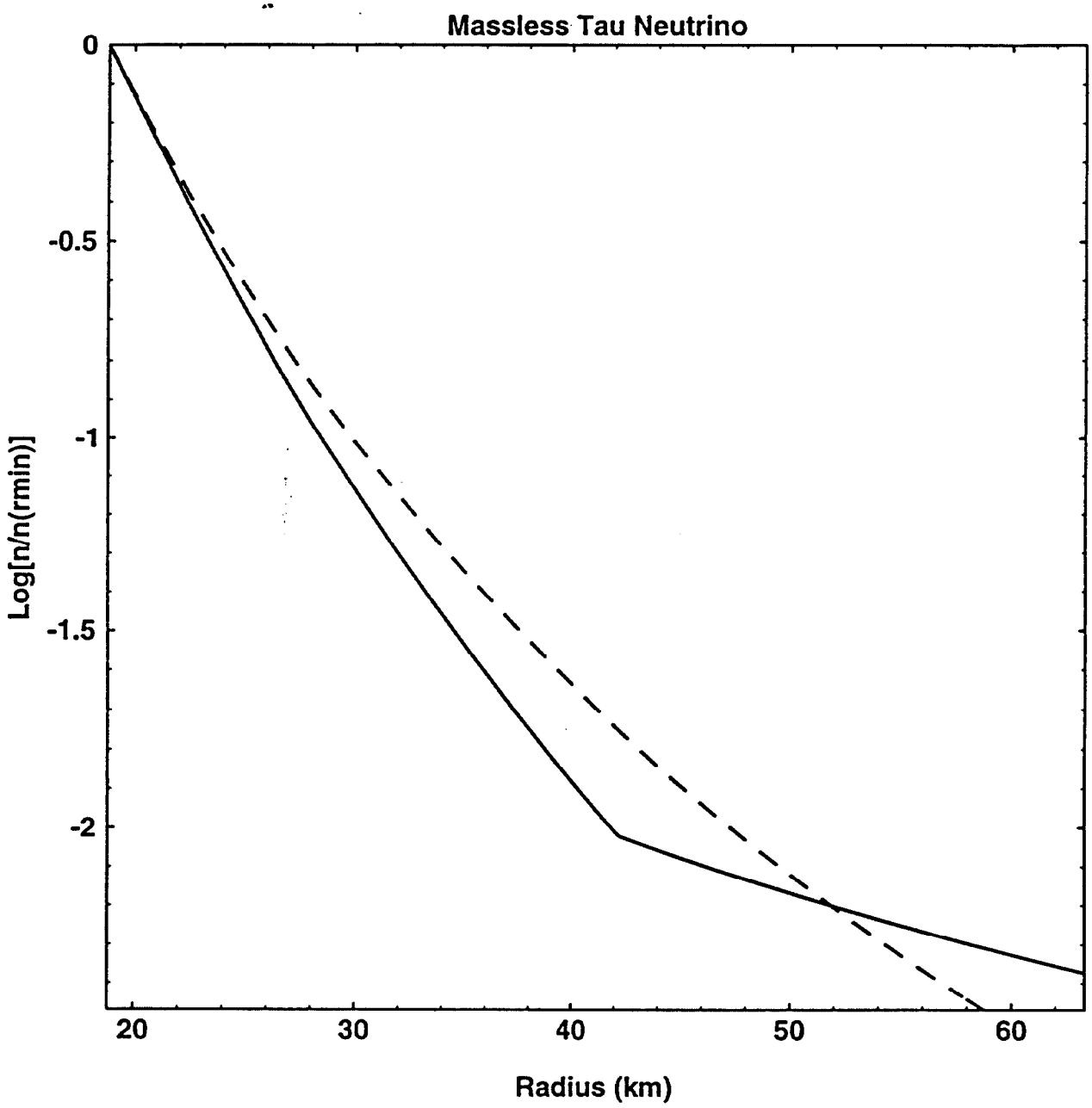
Massless Tau Neutrino
0
-0.5
-1
-1.5
-2
Log[n/n(rmin)]
20
30
40
50
60
Radius (km)

FIG4A

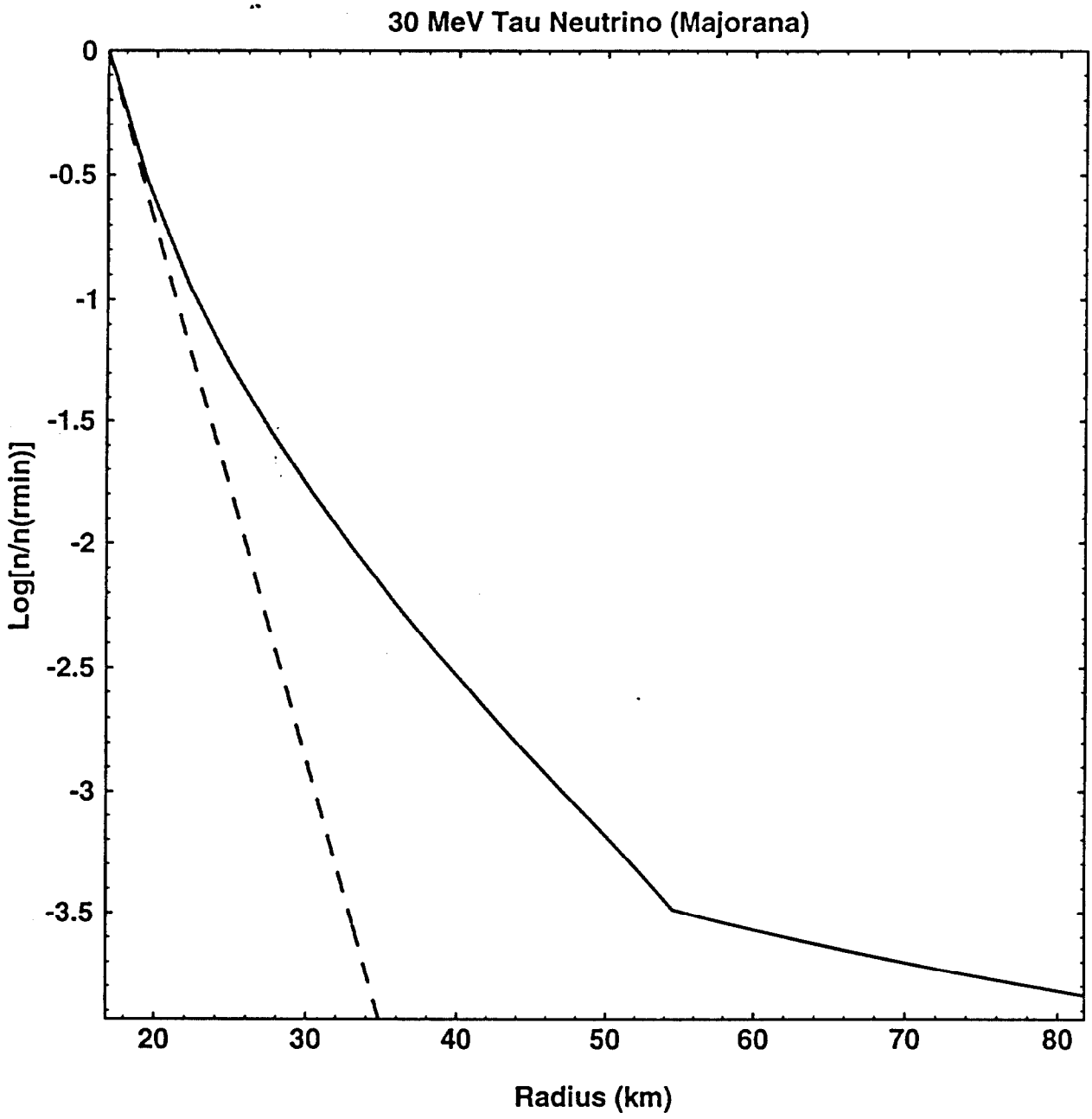
30 MeV Tau Neutrino (Majorana)
0
-0.5
-1
-1.5
-2
-2.5
-3
-3.5
Log[n/n(rmin)]
20
30
40
50
60
70
80
Radius (km)

FIG4B

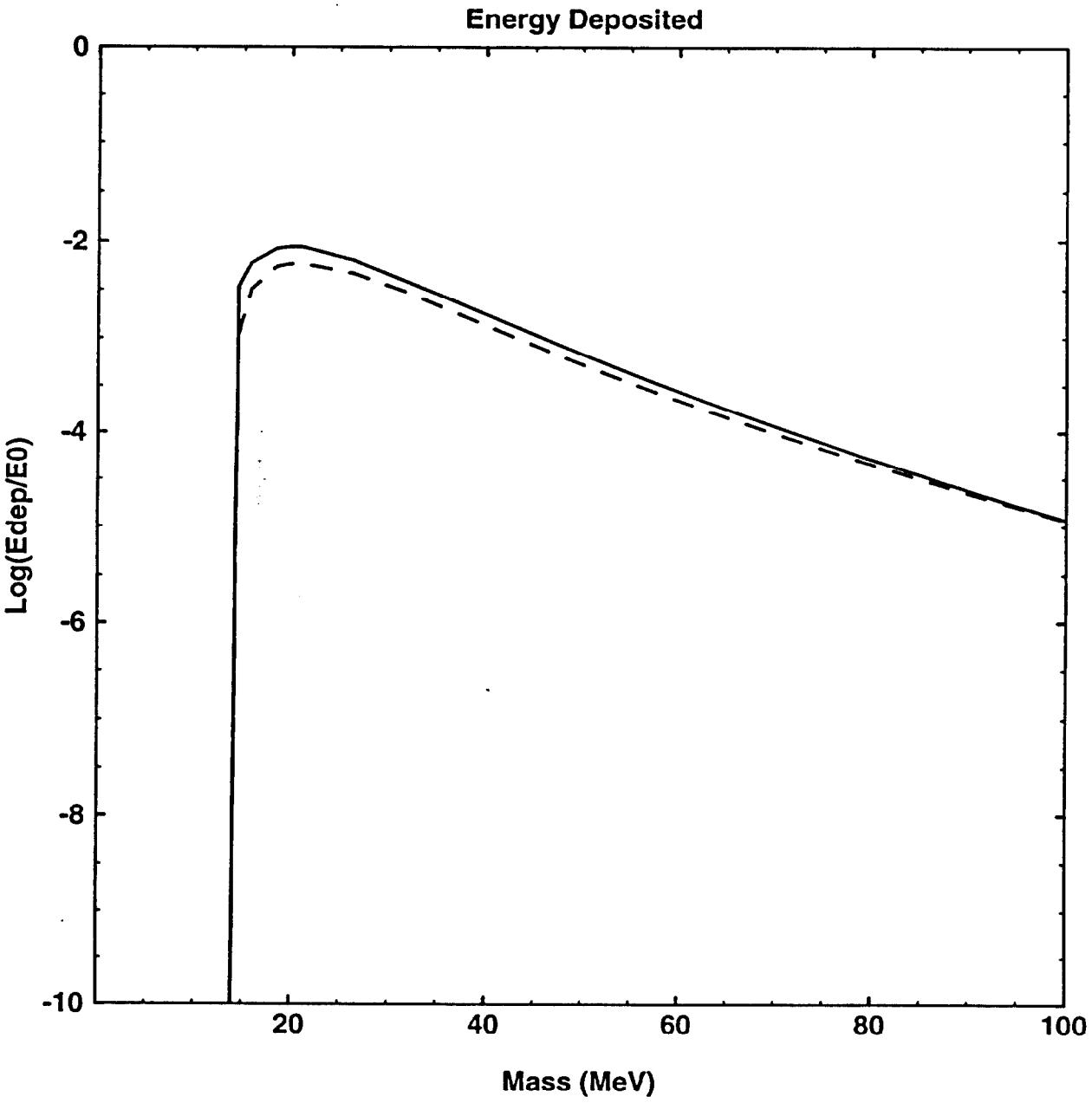

FIG5